

# FAKULTÄT FÜR PHYSIK Praktikum Moderne Physik

Namen: Paul Filip useba[at]student.kit.edu  Namen: Janic Beck  Versuch: Mößbauer-Effekt  Betreuer: Paras Koundal Durchgeführt am: 29.11.20  Wird vom Betreuer ausgefüllt.  1. Abgabe am: Kommentar:
Versuch: Mößbauer-Effekt  Betreuer: Paras Koundal Durchgeführt am: 29.11.20  Wird vom Betreuer ausgefüllt.  1. Abgabe am:
Betreuer: Paras Koundal Durchgeführt am: 29.11.20  Wird vom Betreuer ausgefüllt.
Betreuer: Paras Koundal Durchgeführt am: 29.11.20  Wird vom Betreuer ausgefüllt.
Wird vom Betreuer ausgefüllt.  1. Abgabe am:
1. Abgabe am:
Rückgabe am: Kommentar:
2. Abgabe am:  Ergebnis: + / 0 / - Handzeichen:  Datum: Kommentar:

# Contents

1	The	eory & Preparation					
	1.1	Resonant absorption & Mössbauer effect	1				
	1.2	Mössbauer spectroscopy	2				
2	Ехр	eriment & Evaluation	3				
	2.1	Experimental setup	3				
	2.2	Measuring the 14.4 keV <sup>57</sup> Fe-line	4				
	2.3	Measuring the Mössbauer spectrum	5				
		2.3.1 Iron	5				
		2.3.2 Vacromium					
		2.3.3 FePO <sub>4</sub>	9				
		$2.3.4  \text{FeSO}_4  \dots  \dots  \dots  \dots  \dots  \dots$	11				
	2.4	Conclusion	11				
Bi	bliog	raphy	13				

# 1. Theory & Preparation

#### 1.1 Resonant absorption & Mössbauer effect

The process of **resonant absorption** in nuclear physics describes the phenomenon of de-excitation and subsequent excitation of two similar atoms to the same energy levels via one  $\gamma$ -quant. Consider for example the radioactive decay of  $^{57}$ Co. Via electron capture it transforms into an excited state of  $^{57}$ Fe, which in turn emits a 14.4 keV photon upon deexcitation.

$$^{57}\mathrm{Co} + e^- \longrightarrow ^{57}\mathrm{Fe}^* \qquad ^{57}\mathrm{Fe}^* \longrightarrow ^{57}\mathrm{Fe} + \gamma$$

In principle, due to the symmetry of the latter transition, one could use this emitted photon to raise another <sup>57</sup>Fe atom to the excited state. The photon is absorbed resonantly by the second atom during this process.

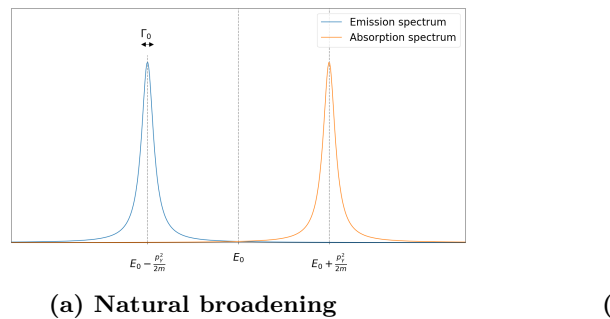
In reality resonant absorption only occurs under certain circumstances. Due to conservation laws the energy  $E_{\gamma}$  of the emitted photon does not exactly equal the transition energy  $E_0$ , but is instead decreased by the nuclear recoil energy. A similar analysis finds that the energy for absorption of the same atom is shifted upwards.

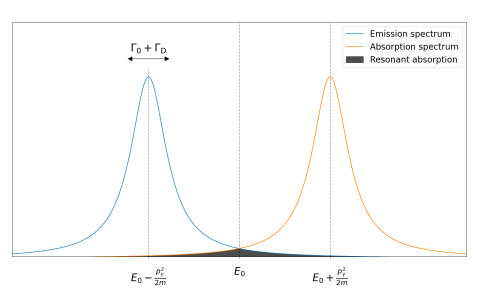
$$\underbrace{E_{\gamma} = E_0 - \frac{p_{\gamma}^2}{2m}}_{\text{Emission}} \qquad \underbrace{E_{\gamma} = E_0 + \frac{p_{\gamma}^2}{2m}}_{\text{Absorption}} \tag{1.1}$$

With the photon impulse  $p_{\gamma}$  and atom mass m. If the line width introduced by natural broadening or other effects does not exceed the recoil energy gap, resonant absorption cannot occur (see Figure 1.1). It is also notable that the energy gap between emission and absorption spectrum can be decreased by additional effects, for example the doppler shift. This will be further discussed in chapter 2.

For optical transitions, the natural linewidth is greater than the recoil energy, so resonance absorption already occurs without external effects. A well-known example is the sodium-D line in the spectrum of visible light. For the  $\gamma$ -transitions, however, it is excluded.

As it turns out, the above rules stating when resonant absorption can and cannot occur are not strictly true. Experiments in the 1960s conducted by R. Mössbauer ([Wer13]) showed that resonant absorption in a crystal lattice happens much more readily than one would expect based on the previous discussion. The difference is the tight binding of the atoms in the crystal lattice. Instead of the individual atom recoiling, different phonons can be created (or destroyed) by the emission and absorption. In a sense, the entire crystal absorbs the recoil energy, effectively substituting the atom mass m in equation Equation 1.1 by the mass M of the entire crystal. Because  $m \ll M$ , the energy gap between emission and absorption spectrum drastically decreases. This phenomenon of recoilless nuclear resonant absorption is named Mössbauer effect.





(b) Natural + Doppler broadening

Figure 1.1: (a) The natural linewidth  $\Gamma_0$  is not sufficient for a sizeable overlap of both spectra. Resonance absorption is not possible. (b) The line width of both spectra can be increase by other effects such as Doppler broadening. In such cases the spectra with linewidth  $\Gamma_0 + \Gamma_D$  can overlap and resonant absorption is possible.

#### 1.2 Mössbauer spectroscopy

To measure the the natural linewidth of <sup>57</sup>Fe with roughly 5 neV¹ common measurement methods will fail. Even with high-resolution interferometers, some orders of magnitude are still missing to resolve such lines by direct measurement of the spectrum. Therefore we take the Mössbauer effect into consideration. It is possible to measure the resonant absorption by the transition rate of the photons. The detector does not need to be energy sensitive, it is sufficient to detect the quanta in this case. The magnitude of the transition displays the overlap of the probabilities for emission and absorption (see Figure 1.1) of the natural lines. By varying the distance of the emission and absorption peaks we can make a statement about the line profile.

If the gamma radiation source is in motion a **Doppler shift** occurs and the photon energy changes. Therefor we can slightly modify the photon energy by changing the velocity of the source (see Equation 1.2).

$$\Delta E_{\gamma} = \pm \frac{v}{c} \cdot E \tag{1.2}$$

With the measured transmission spectrum as a function of the velocity of the source one can make qualitative as well as quantitative statements about the element. Furthermore it is possible to observe three types of nuclear interaction: isometric shift, quadrupole splitting and hyperfine magnetic splitting. The FWHM of the transmission curve corresponds to the double natural linewidth of the transition.

<sup>&</sup>lt;sup>1</sup>[Sch17], Page 160

# 2. Experiment & Evaluation

### 2.1 Experimental setup

The experiment consists of several components. A schematic setup can be seen in Figure 2.1. The  $\gamma$ -source is moving at a velocity relative to the lab frame. The velocity can be adjusted via a digital function generator (DFG), Mössbauer velocity calibrator (MVC), Mössbauer velocity transducer (MVT), and Mössbauer driving unit (MDU). An absorber can be placed in the beam path of the high-energy photons. Based on their energy, resonant absorption occurs and the  $\gamma$ 's are either transmitted or absorbed by the target. The number of transmitted photons is counted by a 1024 channel multi-channel-scaler (MCS). The various other components of the setup (VV, etc.) are used mainly for data acquisition (DAQ) purposes, more detailed information on the individual building blocks can be taken from [Sch17].

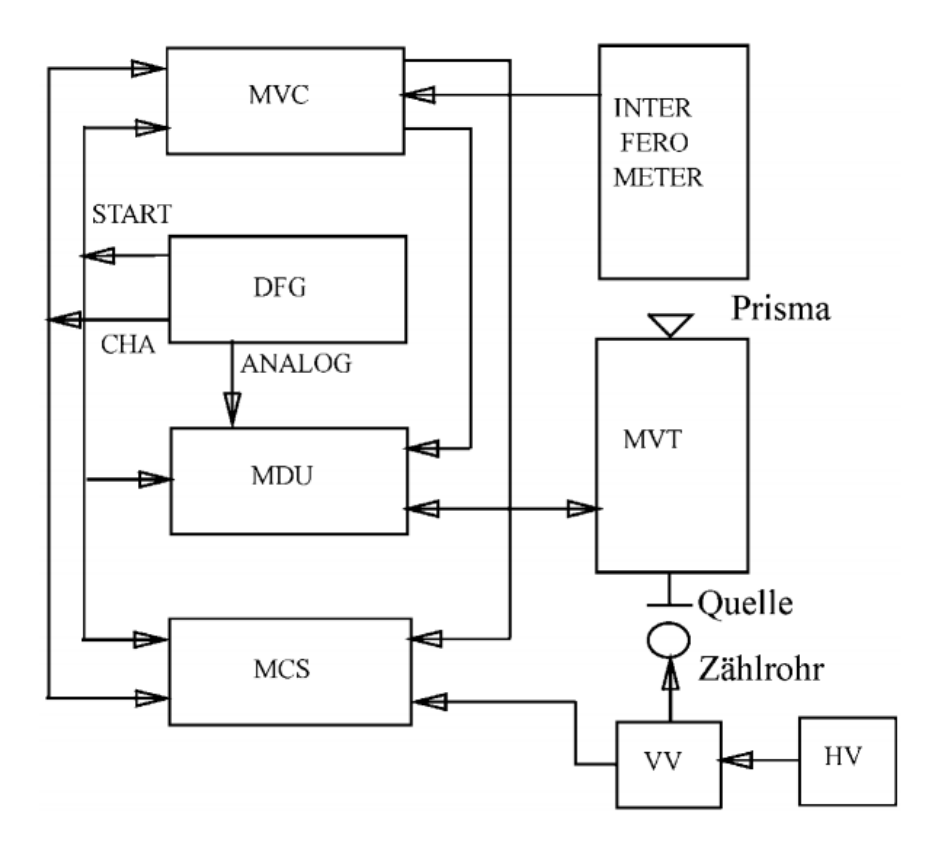


Figure 2.1: A schematic overview of the experiment components. The Mössbauer driving unit (MDU) moves the  $\gamma$ -source at a velocity relative to the multi-channel-scaler (MCS). The exact velocity can be controlled via a digital function generator (DFG), Mössbauer velocity transducer (MVT) and is monitored by an interferometer.

## **2.2** Measuring the $14.4 \,\mathrm{keV}$ <sup>57</sup>Fe-line

As described in section 1.2, Mössbauer spectroscopy does not rely on an extremely precise measurement of the photon energy. Due to resonant absorption it is sufficient to merely count the number of photons transmitted through an absorber to gather information about its atomic energy levels and existing nuclear transitions. However, in order to allow for more detailed analysis in the following evaluation the relative difference of transition energies needs to be quantified. For this purpose as well as a proof of concept, the  $\gamma$ -spectrum of <sup>57</sup>Co is measured. Visible in the observed spectrum in Figure 2.2 is a characteristic Lorentzian peak that reperesents the 14.4 keV resonance of the excited <sup>57</sup>Fe\* state. The exact fit function as well as fit results are given in Equation 2.1. The propagated uncertainty in f is also given.

$$f(\mathcal{C}, A, \omega_0, \gamma) = \frac{A}{(\mathcal{C}^2 - \omega_0^2)^2 + \gamma^2 \omega_0^2}$$
(2.1)

$$A = (8.68 \pm 0.36) \times 10^{10} \tag{2.2}$$

$$\omega_0 = 67.84 \pm 0.08 \tag{2.3}$$

$$\gamma = 23.25 \pm 0.52 \tag{2.4}$$

$$COV(A, \omega_0, \gamma) = \begin{bmatrix} 1.28 \times 10^{19} & 1.00 \times 10^7 & 1.86 \times 10^9 \\ 1.00 \times 10^7 & 5.66 \times 10^{-3} & -6.41 \times 10^{-4} \\ 1.86 \times 10^9 & -6.41 \times 10^{-4} & 2.75 \times 10^{-1} \end{bmatrix}$$

$$\Delta f(\mathcal{C}) = \sqrt{(\nabla f(\mathcal{C}))^T \; \mathrm{COV}(A, \omega_0, \gamma) \; \nabla f(\mathcal{C})}$$

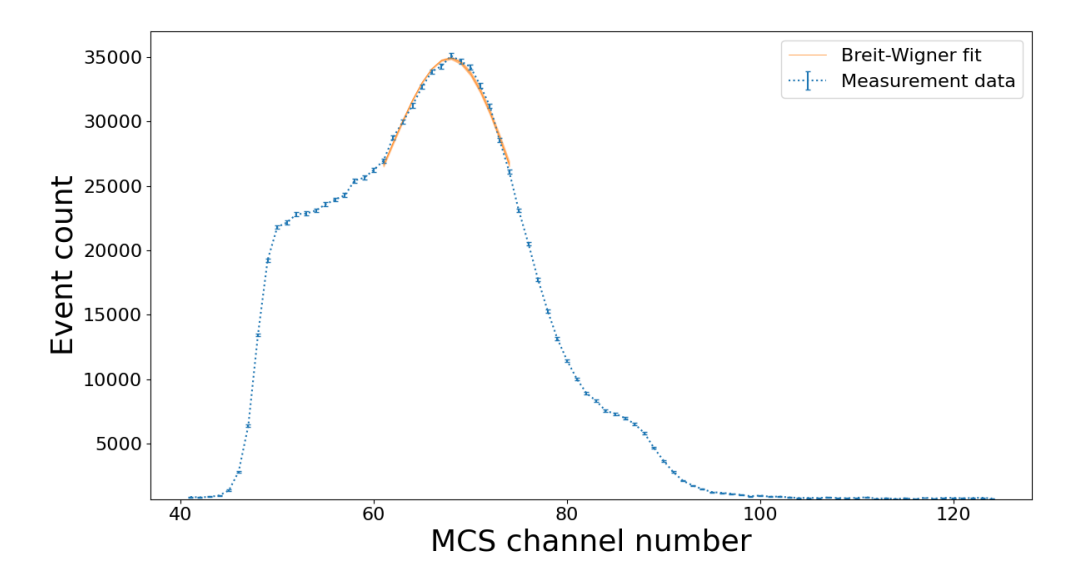


**Figure 2.2:** The error on the measured counts is assumed to be Poissonian. Because the amplitude A does not hold physical information other than the flux of the  $\gamma$ -source, uncertainties and correlations in A are neglected in the below error propagation.

### 2.3 Measuring the Mössbauer spectrum

In the following section the Mössbauer spectrum of various materials is measured. The process of how data is collected and analysed is presented using the example of an iron absorber. Other materials are analysed in a similar fashion.

#### 2.3.1 Iron

The iron absorber is placed in the beam path. The transmitted photons are counted for roughly 20 min. In this measuring mode, the MCS channel number corresponds to a velocity v at which the  $\gamma$ -source is moving relative to the iron target. The 1024 channels available for readout are split into two 512-channel intervals (in the following addressed as Ch1 and Ch2) that differ in the acceleration of the source.It is assumed that the measurements of Ch1 and Ch2 respectively are uncorrelated. As lined out in the lab manual [Sch17] it is assumed that the maximum velocity  $v_{\rm max} = \pm 10 \, \frac{\rm mm}{\rm s}$  corresponds to the edges of the channel intervals (i.e. Channel #0 and #1023 for positive velocity, channel #511, and #512 for negative velocity). Using this information, a relation between channel number  $\mathcal C$  and  $\gamma$ -source velocity can be constructed as follows:

$$v(\mathcal{C}) = 10 \frac{\text{mm}}{\text{s}} \cdot \left(\frac{\mathcal{C} - 256}{256}\right). \tag{2.5}$$

Because of this relative velocity the photons that are emitted at an energy of 14.4 keV are Doppler shifted to slightly lower/higher energies. If now a nuclear transition from state  $|i\rangle$  to state  $|f\rangle$  exists for an iron atom in the crytal lattice where  $E_f - E_i = E'$ , there is a nonzero probability that the atom absorbs the photon and transitions to the higher energy state. Consequently, a dip in the photon spectrum at that specific energy (and by extension a specific velocity) can be observed. The resonance around this energy E' can be modelled by a slightly modified Breit-Wigner shape presented in Equation 2.6.

$$N(v) = \Phi_0 - \frac{A}{(v - v_0)^2 - (\frac{1}{2}\Gamma)^2},$$
(2.6)

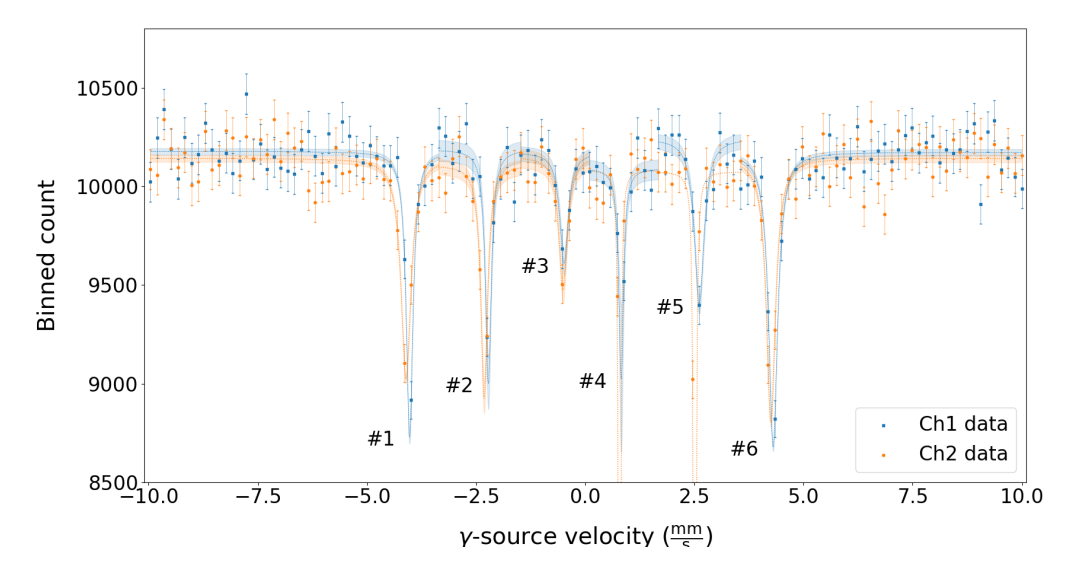


Figure 2.3: Mössbauer spectrum of iron

where  $\Phi_0$  is the integrated  $\gamma$ -flux (i.e. number of photons with energy  $E \approx 14.4\,\mathrm{keV}$ ). The normalisation factor A,  $v_0$  the velocity of the  $\gamma$ -source at which the photons are shifted by the transition energy E' and  $\Gamma$  the full-width-at-half-maximum (FWHM) value of the absorption peak. Technically, using this parametrisation of the Breit-Wigner curve,  $\Gamma$  should also appear in the numerator. To ensure a more stable fit result, it has however been absorbed in A.

Fitting Equation 2.6 to measurement data, six absorption peaks can be identified (see Figure 2.3) depending on the velocity of the  $\gamma$ -source. The individual parameters optimised to model the observed spectrum are listed in Table 2.1. It is important to note that absorption peak #4 and #5 are not properly fitted for data from Channel 2. The information gathered from these peaks will be ignored in the following analysis. For every other absorption peak the corresponding fit parameters P will be combined to a mean value  $\bar{P}$ .

$$\bar{P} = \frac{1}{2} \left( P_{\text{Ch1}} + P_{\text{Ch2}} \right)$$

$$\Delta \bar{P} = \frac{1}{2} \sqrt{\Delta P_{\mathrm{Ch1}}^2 + \Delta P_{\mathrm{Ch2}}^2}$$

Due to the use of different emitter and absorber materials, a **isomer shift** occurs. This is caused by the different charge radii and electron distribution of the states involved in the transition. In the Mößbauer spectrum this results in a fixed shift of all absorption peaks around the center (v=0), which overlaps with other phenomena. The isomer shift can be calculated by determining the center of gravity of pairwise connected lines.

At the <sup>57</sup>Co-Rh source with natural iron as absorber an isomer shift of

$$\Delta E = (6.80 \pm 0.12) \cdot 10^{-9} \text{eV}$$
 (2.7)

occurs.

Another effect is the **hyper fine splitting** of <sup>57</sup>Fe. This is caused by the movement of the shell electrons and a resulting magnetic field B at the location of the atomic nucleus. Due

Peak #	$\Phi_0$	A	$v_0$	Γ	Channel
#1	$10177 \pm 16$	$12 \pm 3.9$	$-4.02 \pm 0.02$	$0.184 \pm 0.043$	Ch1
#1	$10142 \pm 17$	$21 \pm 6.0$	$-4.11 \pm 0.02$	$0.277\pm0.049$	$\mathrm{Ch}2$
#2	$10187 \pm 53$	$8 \pm 6.2$	$-2.22\pm0.03$	$0.161\pm0.104$	Ch1
<del># 2</del>	$10108 \pm 38$	$10 \pm 5.6$	$-2.32\pm0.01$	$0.184 \pm 0.080$	Ch2
#3	$10173 \pm 37$	$8 \pm 5.2$	$-0.49 \pm 0.02$	$0.234\pm0.099$	Ch1
<del>#</del> 5	$10151 \pm 47$	$9 \pm 5.6$	$-0.51 \pm 0.03$	$0.235\pm0.076$	Ch2
#4	$10092 \pm 50$	$4\pm6.0$	$0.82 \pm 0.02$	$0.130\pm0.193$	Ch1
#±	$10082 \pm 65$	$2 \pm 6.1$	$0.79 \pm 0.05$	$0.000 \pm \infty$	Ch2
#5	$10243 \pm 38$	$15 \pm 5.4$	$2.61 \pm 0.02$	$0.266\pm0.048$	Ch1
<del>#</del> 0	$10075 \pm 24$	$3 \pm 2.4$	$2.51 \pm 0.02$	$0.000 \pm \infty$	Ch2
#6	$10173 \pm 17$	$23 \pm 5.1$	$4.30 \pm 0.01$	$0.246 \pm 0.036$	Ch1
<del></del> 0	$10142 \pm 19$	$21 \pm 6.9$	$4.25 \pm 0.01$	$0.250 \pm 0.058$	Ch2

Table 2.1: Mössbauer spectrum fit parameters for iron

to the Zeeman effect the degenerated state of the nucleus splits into 2I+2 levels. I is the nuclear spin and there are 2I+1 possible values of the magnetic quantum number m. The energy distances are given by

$$\Delta E_m = -\frac{m}{I}\mu B. \tag{2.8}$$

It follows for the energy of the  $\gamma$ -quanta with resonance absorption, considering the hyperfine splitting of excited (index a) and ground state (index g):

$$E_{\gamma} = E_0 - \frac{m_a}{I_a} \mu_a B + \frac{m_g}{I_g} \mu_g B \tag{2.9}$$

The excited state  $I_a = \frac{3}{2}$  is split fourfold and the basic state  $I_g = \frac{1}{2}$  is split twice. For dipole transitions, however, the selection rule  $\Delta m = m_a - m_g = 0 \pm 1$  applies, so only six transitions are permitted. The magnetic moment of the ground state is already known with

$$\mu_g = (0.0903 \pm 0.0007) \,\mu_k \tag{2.10}$$

where  $\mu_k = \frac{e\hbar}{2m_p}$  corresponds to the nuclear magneton. Thus, the internal magnetic field and the magnetic moment of the excited state,  $\mu_a$ , can be determined.

The complete derivation of the calculation is in the blue book and is therefore only outlined here. The six possible transitions can be described by the newly defined sizes A, G and  $I_0$ . These are given by:

$$A = \frac{\mu_a Bc}{I_a E_0} \qquad G = \frac{\mu_g Bc}{I_a E_0} \tag{2.11}$$

where  $I_0$  corresponds to the isomer shift already calculated.  $E_0 = (14.40 \pm 0.05) \,\text{keV}$  is the energy of the ground state and c is the velocity of light. There are four cases to distinguish, depending on the relative size of the unknowns to each other. The case with the smallest deviation is chosen.

	Ch1 in $10^{-3} \frac{\text{m}}{\text{s}}$	Ch2 in $10^{-3} \frac{\text{m}}{\text{s}}$
$v_1$	4.16	4.11
$v_2$	2.48	2.38
$v_3$	0.69	0.65
	-1.47	-1.29
$v_1 - 2v_2 + v_3 = 0$	-0.10	0.01
$v_1 - v_2 - 2v_3 = 0$	0.32	0.44
$-v_1 + v_2 + 2v_3 = 0$	-0.32	-0.44

Table 2.2: Case distinction in the calculation of hyperfine structure splitting

**Table 2.3:** Inner magnetic field and magnetic moment of the excited <sup>57</sup>Fe state.

	Ch1	Ch2	Mean
Inner magnetic field	$-(26.71 \pm 0.39)\mathrm{T}$	$-(25.54 \pm 0.45)\mathrm{T}$	$-(26.12 \pm 0.71) \mathrm{T}$
Magnetic moment	$-(4.56 \pm 0.15) \cdot 10^{-9} \text{eV}$	$-(4.91 \pm 0.16) \cdot 10^{-9} \text{eV}$	$-(4.73 \pm 0.23) \cdot 10^{-9} \text{eV}$

(a) 
$$v_1 - 2v_2 - v_3 = 0$$

(b) 
$$v_1 - 2v_2 + v_3 = 0$$

(c) 
$$v_1 - v_2 - 2v_3 = 0$$

(d) 
$$-v_1 + v_2 + 2v_3 = 0$$

The velocities  $v_1 > v_2 > v_3$  correspond to the positive absorption peaks of the Mößbauer spectrum and are already corrected for the isomer shift.

The slightest deviation therefore occurred in case two (see Table~2.2). From this follows for the unknowns:

$$A = v_1 - v_2 G = -v_2 - v_3. (2.12)$$

By transforming the equations (Equation 2.11 and Equation 2.12) follows:

$$\mu_a = \frac{AI_a E_0}{Bc} = \frac{(v_1 - v_2)I_a E_0}{Bc} \qquad B = \frac{GI_g E_0}{\mu_g c} = \frac{(-v_2 - v_3)I_g E_0}{\mu_g c}$$
(2.13)

where the magnetic field B is used in the first equation. Thus the inner magnetic field and the magnetic moment of the excited state are given by  $Table\ 2.3$ .

### 2.3.2 Vacromium

Next, a vacromium absorber is placed in the beam path<sup>1</sup>. The analysis of data proceeds as presented in subsection 2.3.1. One absorption peak can be discovered in the vacromium Mössbauer spectrum as seen in Figure 2.4 and Table 2.4.

The isometric shift for Vacromium can be determined in the same way it was determined for iron in subsection 2.3.1. The isometric shift of the absorption peaks is hence

$$\Delta E = (10.380 \pm 1.652) \times 10^{-9} \,\text{eV}$$
 (2.14)

<sup>&</sup>lt;sup>1</sup>The vacromium Mössbauer spectrum was measured last (and longest) during the lab exercise. In order to streamline the text it is however decided to discuss the material in this section already.

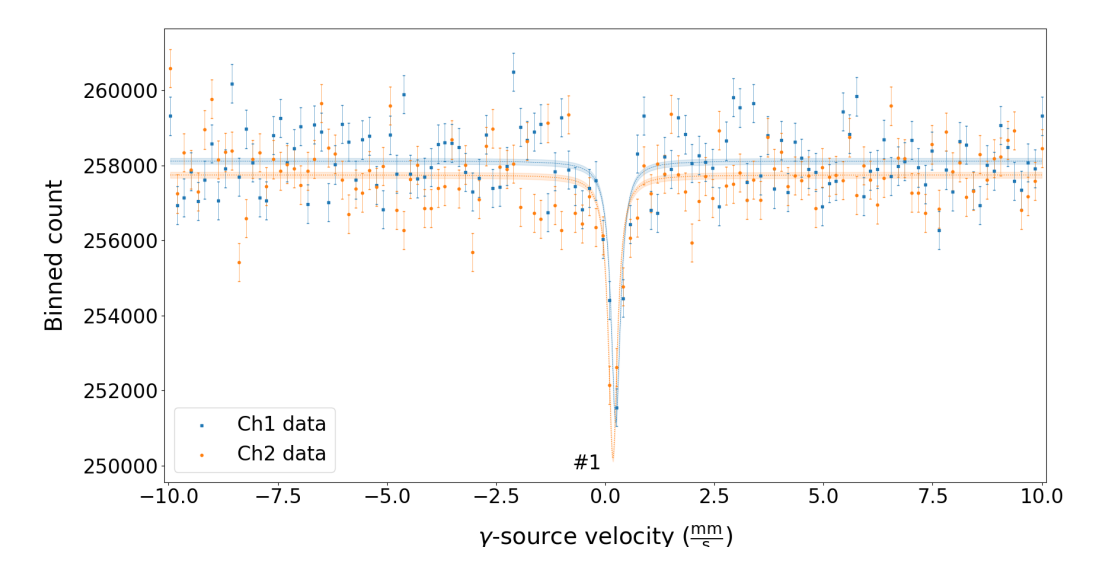


Figure 2.4: Mössbauer spectrum of vacromium

Table 2.4: Mössbauer spectrum fit parameters for vacromium

Peak #	$\Phi_0$	A	$v_0$	Γ	Channel
	$258122 \pm 78$	$120 \pm 39.1$	$0.24 \pm 0.03$	$0.262 \pm 0.050$	Ch1
#1	$257749 \pm 80$	$120 \pm 54.1$	$0.18 \pm 0.01$	$0.252 \pm 0.082$	Ch2

The FWHM for Ch1 and Ch2 in terms of photon energy caused by the Doppler shift is

$$\Gamma_{\rm Ch1} = (5.250 \pm 1.009) \times 10^{-9} \, {\rm eV}$$
  
 $\Gamma_{\rm Ch2} = (5.041 \pm 1.644) \times 10^{-9} \, {\rm eV}.$ 

It follows a mean value of  $\Gamma = (5.146 \pm 0.965) \times 10^{-9}$  eV. From this the mean lifetime  $\tau$  of the metastable 14.4 keV <sup>57</sup>Fe-state is given by the time-energy uncertainty relation.

$$\tau \cdot \Gamma = \hbar \Leftrightarrow \tau = \frac{\hbar}{\Gamma} = (127.91 \pm 23.98) \,\text{ns}$$
 (2.15)

This lies within the expectation of a literature value  $\tau = 141$  ns extracted from [NHT81].

#### 2.3.3 FePO<sub>4</sub>

The third absorber that is placed in the  $\gamma$ -source beam path is the iron compound FePO<sub>4</sub>. The Mössbauer spectrum of FePO<sub>4</sub> displays two characteristic absorption peaks that are closely located. This is shown in Figure 2.5. The fit parameters of the optimisatisation are given in Table 2.5.

The isometric shift of FEPO<sub>4</sub> is given by Equation 2.16 and has again been calculated in the same process as lined out in subsection 2.3.1.

$$\Delta E = -(103.040 \pm 6.571) \times 10^{-10} \,\text{eV}.$$
 (2.16)

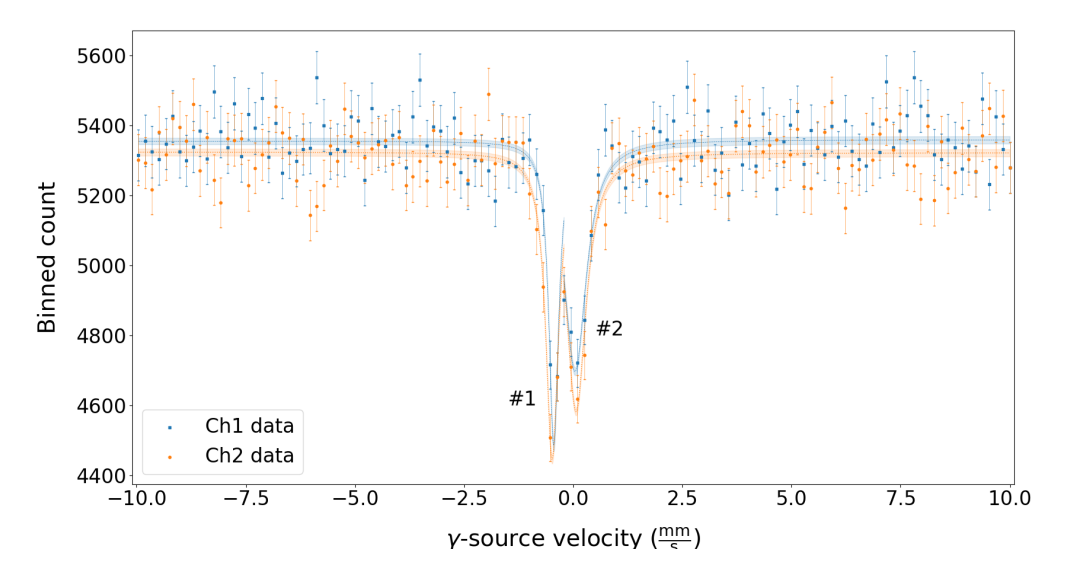


Figure 2.5: Mössbauer spectrum of FePO<sub>4</sub>

In an attempt to quantify the electric field gradient  $\frac{\partial E}{\partial z} = \frac{\partial^2 V}{\partial z^2}$  along the axis of the permeating magnetic field, the number of and distance between absorption peaks is analysed in more detail. These observables are influenced by the **quadrupole** shift. Following the derivation in [Sch17], the energy by which a state with nuclear spin I and magnetic moment m, and electric quadrupole moment Q is altered calculates as

$$\Delta E_Q(I, m) = \frac{e \cdot Q}{4} \frac{3m^2 - I \cdot (I - 1)}{3I^2 - I \cdot (I + 1)} \frac{\partial^2 V}{\partial z^2}.$$
 (2.17)

Owed to the material properties of FePO<sub>4</sub> and FeSO<sub>4</sub> in the following subsection, and taking into account the Doppler shift of the high-energy  $\gamma$ 's, Equation 2.17 can be rewritten so that the electric field gradient can be obtained from the location v of absorption peaks.

$$\Delta E_Q(\frac{3}{2}, \pm \frac{3}{2}) = + \frac{e \cdot Q}{4} \frac{\partial^2 V}{\partial z^2}, \qquad \Delta E_Q(\frac{3}{2}, \pm \frac{1}{2}) = - \frac{e \cdot Q}{4} \frac{\partial^2 V}{\partial z^2}$$

$$\begin{split} \Delta v &= v(\frac{3}{2}, \pm \frac{3}{2}) - v(\frac{3}{2}, \pm \frac{1}{2}) = \frac{e \cdot Q}{2} \cdot \frac{c}{E_0} \cdot \frac{\partial^2 V}{\partial^2 z} \\ \Leftrightarrow & \quad \frac{\partial^2 V}{\partial^2 z} = \frac{2E_0}{e \cdot Q \cdot c} \ \Delta v. \end{split}$$

With the given quadrupole moment  $Q=(0.21\pm0.01)\times10^{-28}\,\mathrm{m}^2$  from [Sch17]and the location of the absorption peaks as listed in Table 2.5, the electric field gradient is found to be

$$\frac{\partial^2 V}{\partial^2 z} = (2.3673 \pm 0.1490) \times 10^{24} \, \frac{V}{m^2}.$$
 (2.18)

This corresponds to an electric field strength of roughly  $2.36 \times 10^{14} \frac{V}{m}$  across characteristic length scales of an atom (  $10^{-10}$  m).

Peak $\#$	$\Phi_0$	A	$v_0$	$\Gamma$	Channel
#1	$5355 \pm 9$	$16 \pm 7.1$	$-0.45 \pm 0.01$	$0.275 \pm 0.080$	Ch1
<del>//</del> 1	$5323 \pm 10$	$28 \pm 7.4$	$-0.48 \pm 0.02$	$0.358\pm0.057$	$\mathrm{Ch}2$
#2	$5359 \pm 11$	$64 \pm 17.9$	$0.04 \pm 0.03$	$0.622 \pm 0.103$	Ch1
<del>#</del> 2	$5322 \pm 10$	$57 \pm 13.9$	$0.06 \pm 0.02$	$0.557 \pm 0.080$	Ch2

Table 2.5: Mössbauer spectrum fit parameters for phosphate

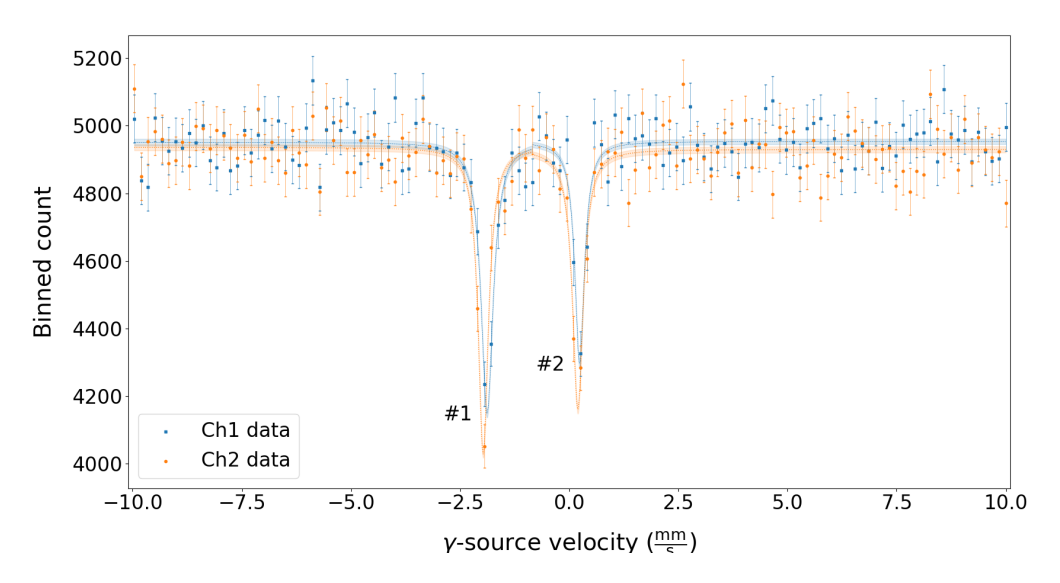


Figure 2.6: Mössbauer spectrum of FeSO<sub>4</sub>

#### $2.3.4 \text{ FeSO}_4$

Lastly, the Mössbauer spectrum of  $FeSO_4$  is evaluated under the same aspects as the previous samples. Only the results gathered from analysis will be listed here. For a discussion of systematics and more information how the analysis is conducted earlier sections of this lab report can be referred to. Overall, two absorption peaks are visible in the Mössbauer spectrum of  $FeSO_4$  (See Figure 2.6 and Table 2.6).

The energetic shift of the absorption peaks caused by isomeric shift is

$$\Delta E = (-42.74 \pm 1.52) \times 10^{-9} \,\text{eV}.$$
 (2.19)

The electric field gradient is calculated as

$$\frac{\partial^2 V}{\partial^2 z} = (9.789 \pm 0.517) \times 10^{24} \, \frac{V}{m^2}.$$
 (2.20)

### 2.4 Conclusion

The physics of the Mössbauer effect were tested experimentally. Different characteristics of the various absorbers - such as their isometric shift - were quantified. Where possible, the obtained values are compared to values given by literature. Overall, the analysis

Γ Peak #  $\Phi_0$ AChannel  $v_0$  $-1.88 \pm 0.01$  $4951 \pm 10$  $22 \pm 5.6$  $0.334\pm0.053$ Ch1 #1  $4936 \pm 9$  $-1.97 \pm 0.01$ Ch2  $18 \pm 3.4$  $0.281 \pm 0.032$  $4953 \pm 8$  $11\pm3.0$  $0.24 \pm 0.02$  $0.264 \pm 0.041$ Ch1 #2  $4930 \pm 9$  $17 \pm 5.0$  $0.20 \pm 0.01$  $0.299 \pm 0.057$ Ch2

Table 2.6: Mössbauer spectrum fit parameters for sulfate

largely conforms to established theory. However, large relative errors are found for all the listed measurement parameters. These are largely caused by statistical uncertainties of the Mössbauer spectrum fit parameters. In future lab reports these could be diminished by using more powerful fitters than were used in this analysis (numpy, scipy). Another promising idea is a combined analysis of the whole Mössbauer spectrum, rather than fitting individual to absorption peaks. In theory, the fit parameters  $\Phi_0$  or the normalisation parameter A should be the same for the different peaks. Using this knowledge, one could construct a fit function that optimises these values globally and then fits the location and FWHM of the absorption peaks. This might result in a more stable fit.

# Bibliography

- [NHT81] Nishida, Tetsuaki, Toshiharu Hirai und Yoshimasa Takashima: *Moessbauer spectroscopic study of potassium borosilicate glasses at low temperatures*. Bulletin of the Chemical Society of Japan, 54(12):3735–3738, 1981.
- [Sch17] Schmidt, F.K.: Einführung in das Kernphysikalische Praktikum. Institut für Experimentelle Kernphysik, Karlsruhe, Ausgabe Oktober 2017.
- [Wer13] Wertheim, Gunther K: Mössbauer effect: principles and applications. Academic Press, 2013.